Review

Not peer-reviewed version

Diagnostic Accuracy of Blood Flow Dependent Imaging in Diagnosing Thyroid Neoplasms: A Network Systematic Review and Meta-Analysis

Dev Desai , Maria Eleni Malafi , Abhijay Shah , Anushka Verma , Aarya Naik , Hetvi Shah *

Posted Date: 21 December 2023

doi: 10.20944/preprints202312.1669.v1

Keywords: Thyroid Nodule; Radionuclide Scanning; Superior Microvascular Imaging; Color Doppler Diagnosis; Sensitivity; Specificity; Diagnostic imaging

Review

Diagnostic Accuracy of Blood Flow Dependent Imaging in Diagnosing Thyroid Neoplasms: A Network Systematic Review and Meta-Analysis

Dev Desai MBBS [1], Maria Eleni Malafi [2], Abhijay Shah MBBS [3], Anushka Verma MBBS [4], Dr. Aarya Naik MBBS [5] and Hetvi Shah MBBS [6,*]

[1] SMT. NHLMMC, Ahmedabad, India; Devhdesai01@gmail.com
[2] Medical School, Democritus University of Thrace, Alexandroupoli, Greece; marilenmalafi@gmail.com
[3] SMT. NHLMMC, Ahmedabad, India; abhijayshah0610@gmail.com
[4] SMT. NHLMMC, Ahmedabad, India; anushkasinghverma@gmail.com
[5] SMT. NHLMMC, Ahmedabad, India; aaryanaik1999@gmail.com
[6] SMT. NHLMMC, Ahmedabad, India
* Correspondence: Shahhetvi1026@gmail.com

Abstract: Background: Thyroid nodules are common, affecting nearly 65% of the general population. While they are widespread, it's crucial to recognize that the majority of these nodules are not cancerous and can be effectively managed through careful monitoring. Thyroid ultrasound is commonly used to evaluate thyroid nodules owing to its low cost, wide availability and technical ease of application. In sonography, it's crucial to assess characteristics and vascular flow. Yet, conventional color and power Doppler ultrasound may not always effectively capture small vessels and low velocities due to their limitations. Superior Microvascular Imaging can display the blood flow of small vessels and low-velocity blood flow, which is difficult to visualize with conventional Doppler ultrasound. Meanwhile other thyroid scans, that utilize either [99mTc] pertechnetate or (18)F-fluorodeoxyglucose, can categorize nodules as hyperactive ('hot'), exhibiting normal activity ('warm'), or having reduced/no activity ('cold'). Thus, the main goal of screening and tracking thyroid nodules is to improve the management of potentially worrisome thyroid malignancies. **Methodology:** The study was conducted within the structural framework of a network meta-analysis, with the index tests being - SMI, Radionuclide Scanning and Color Doppler, and the general link between them being the reference gold standard. The data collection involved searching for all pertinent literature using PubMed, Google Scholar, and the Cochrane Library databases. The essential data was extracted following the application of specific inclusion and exclusion criteria. This meta-analysis included 7 RCTs with 1,152 patients for Radionuclide Scanning, 10 RCTs with 1,847 patients for SMI and 8 RCTs with 4,480 patients for Color Doppler. They were analyzed using the QualSyst tool and the risk of bias was evaluated by using QUADAS-2 analysis. The statistical software packages MetaDiSc 1.4, RevMan (Review Manager, version 5.3), SPSS (Statistical Package for the Social Sciences, version 20) and Excel in Stata 14 were used to perform the statistical analyses. **Result:** According to the findings, the sensitivity for Radionuclide Scanning is calculated as 0.79 (range: 0.76 to 0.81) and specificity as 0.55 (range: 0.50 to 0.60) with a 95% confidence interval. The overall diagnostic odds ratio (DOR) for Radionuclide Scanning Is 10.54. Additionally, with a 95% confidence interval, SMI exhibits a sensitivity of 0.82 (with a range of 0.79 to 0.84) and a specificity of 0.86 (with a range of 0.84 to 0.88), while the overall DOR is approximately 25.73. Color Doppler demonstrates a calculated sensitivity of 0.71 (ranging from 0.69 to 0.74) and specificity of 0.81 (ranging from 0.79 to 0.83) with a 95% confidence interval, while its DOR is 13.48. **Conclusion:** As evidenced by this meta-analysis, blood flow dependent imaging techniques are superior in their abilities to be used as diagnostic tests, especially in conjunction with their use in detecting thyroid nodules. This study offers a starting point for delving deeper into the utilization of Radionuclide Imaging, Superior Microvascular Imaging and Color Doppler in diagnosing thyroid nodules in a clinical setting.

 doi:10.20944/preprints202312.1669.v1

Keywords: Thyroid Nodule; Radionuclide Scanning; Superior Microvascular Imaging; Color Doppler Diagnosis; Sensitivity; Specificity; Diagnostic imaging

---

Introduction

Thyroid imaging includes several types of tests that provide information about the structure and function of the thyroid gland. These tests are used to diagnose problems with the thyroid gland, such as hyperthyroidism, cancer, or other growths.

The most common types of thyroid imaging tests are thyroid scans and radioactive iodine uptake tests.

A thyroid scan is a nuclear medicine examination that uses the emissions of gamma rays from radioactive iodine to help determine whether a patient has thyroid problems, including hyperthyroidism, cancer, or other growths.

A radioactive iodine uptake test (RAIU) is also known as a thyroid uptake. It is a measurement of thyroid function, but does not involve imaging. The thyroid scan and thyroid uptake provide information about the structure and function of the thyroid.(1)

A whole-body thyroid scan is typically performed on people who have or had thyroid cancer. During a thyroid scan, the scanner detects the location and intensity of the gamma rays emitted by the radioactive iodine, and the computer displays images of the thyroid gland.

Other scans use a substance called technetium instead of radioactive iodine. The thyroid uptake and scan play a central role in the diagnosis of thyroid diseases and abnormalities in thyroid function as it provides detailed information.(2)

The widespread use of ultrasound in diagnosis and management of thyroid disorders can be attributed to its low cost, wide availability and technical ease of application.(3)

Blood flow dependent thyroid imaging involves ultrasound imaging techniques being applied to assess blood circulation within the thyroid.

Thyroid ultrasound is commonly used to evaluate thyroid nodules. The use of high frequency sound waves produces an image of the gland which can provide information about the shape and structure of the nodules.(4)

Ultrasound can distinguish cysts from solid nodules or determine if multiple nodules are present. It can also distinguish cysts from solid nodules and determine if multiple nodules are present. It may also be used as a guide when performing fine-needle aspiration biopsies.(5)

Another imaging process that uses ultrasound as its basis is Color flow Doppler Sonography (CFDS). CFDS is particularly useful to distinguish between untreated Graves' disease and Hashimoto's thyroiditis, as it reveals a significantly greater increase in blood flow in Graves disease. It is also important to note that thyroid vascularity and blood flow do not rely on serum thyroid hormone levels, but are notably elevated in untreated Graves disease, indicating excessive thyroid stimulation by the TSH-receptor antibodies.(6) Heightened thyroid blood flow encompasses increased thyroid artery diameter, increased flow velocity and a reduction in peripheral resistance.(7)

Preprints.org (www.preprints.org) | NOT PEER-REVIEWED | Posted: 21 December 2023 doi:10.20944/preprints202312.1669.v1

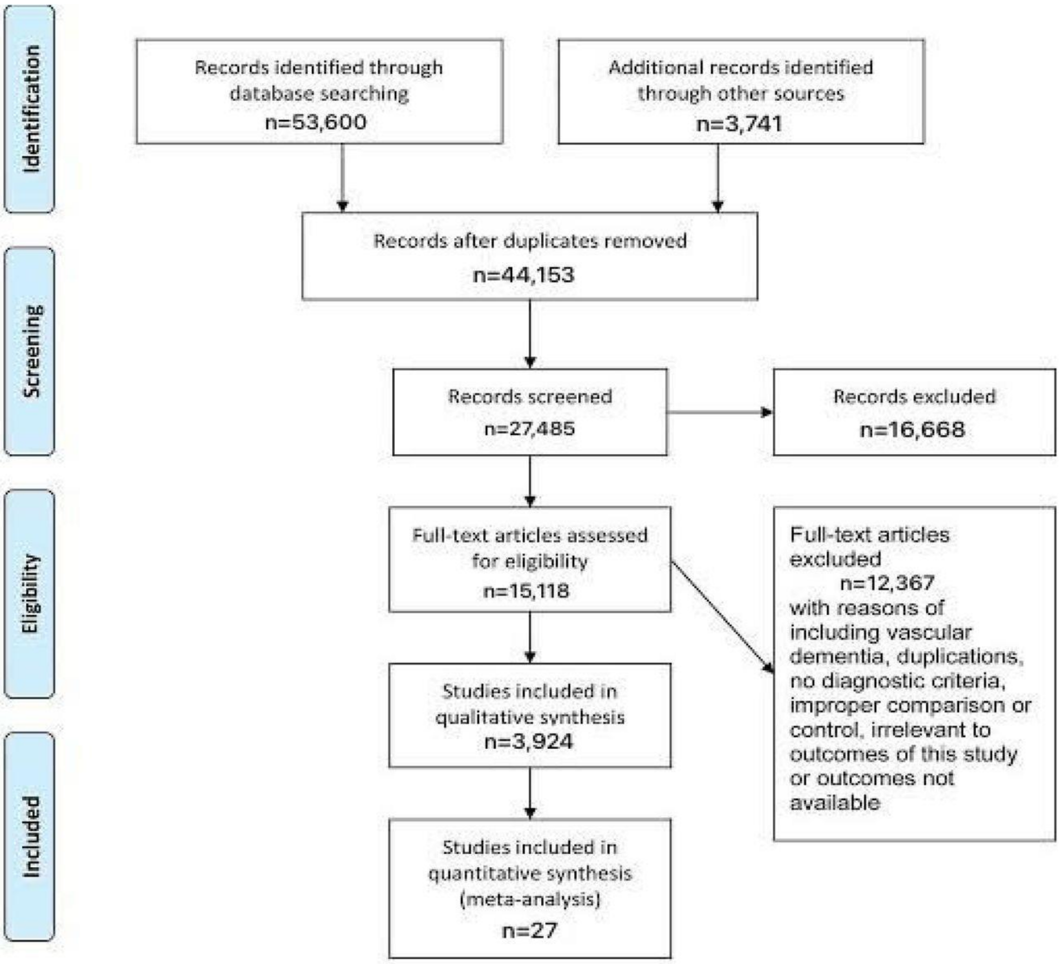

Figure 1. Prisma Flowchart.

Methodology

The study was conducted within the structural framework of a network meta-analysis, with the index tests being - SMI, Radionuclide Scanning and Color Doppler, and the general link between them being the reference gold standard.

Preprints.org (www.preprints.org) | NOT PEER-REVIEWED | Posted: 21 December 2023 doi:10.20944/preprints202312.1669.v1

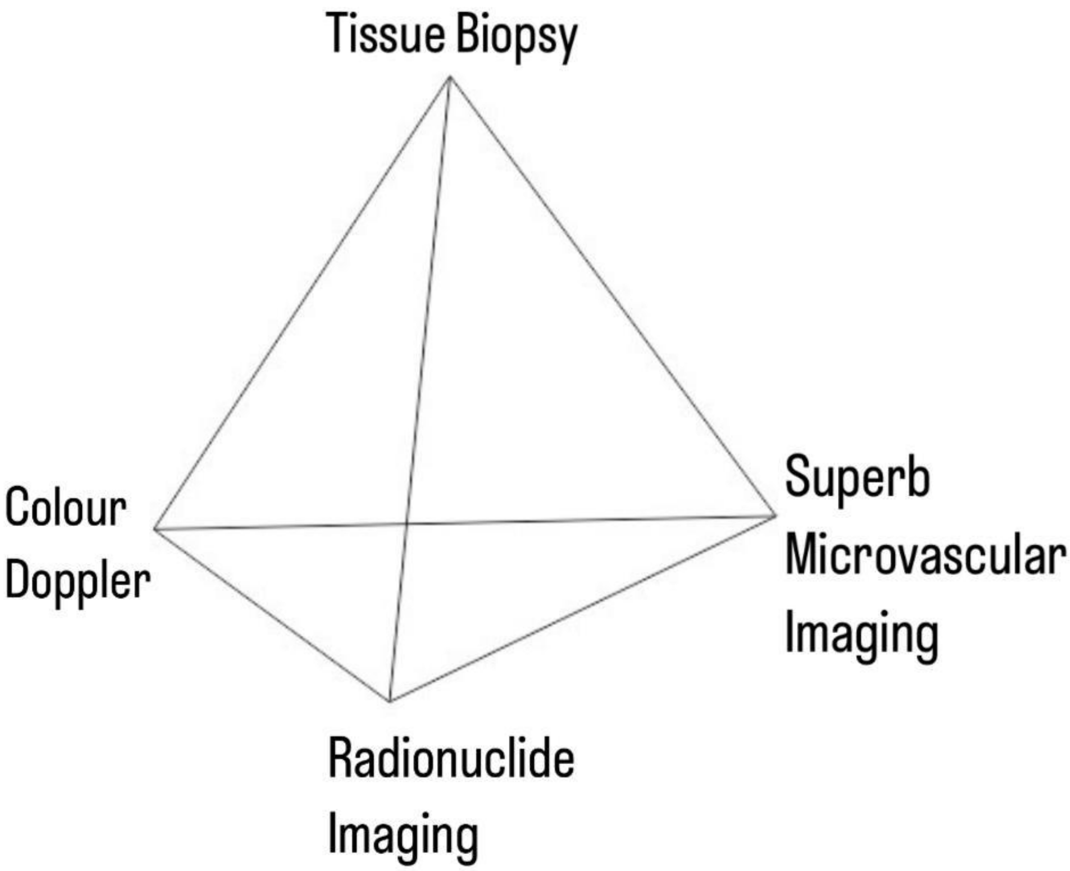

Figure 2. Network Pyramid.

Data Collection

For the collection of the data, a search was done by two individuals using PubMed, Google Scholar, and Cochrane Library databases for all relevant literature. Full - Text Articles written only in English were considered.

The medical subject headings (MeSH) and keywords, 'Thyroid Nodule', 'Superb Microvascular Imaging', 'Color Doppler', 'Radionuclide Scan' and 'Thyroid Perfusion' were used. References, reviews, and meta-analyses were scanned for additional articles.

Inclusion and Exclusion Criteria

Titles and abstracts were screened, and duplicates and citations were removed. References of relevant papers were reviewed for possible additional articles. Papers with detailed patient information and statically supported results were selected.

Preprints.org (www.preprints.org) | NOT PEER-REVIEWED | Posted: 21 December 2023 doi:10.20944/preprints202312.1669.v1

We searched for papers that show more accurate diagnoses, where modalities considered were Superb Microvascular Imaging (SMI), Color Doppler (CD) and Radionuclide Scanning for detection of thyroid nodules.

The inclusion criteria were as follows: (1) Studies that provided information about the accurate diagnosis with aforementioned modalities; (2) Studies published after the year 2000; (3) Studies comparing aforementioned modalities amongst each other well as comparisons to the Gold Standard (biopsy) as a diagnosis modality for cases of thyroid nodules.

The exclusion criteria were: (1) articles that were not full text, (2) unpublished articles, and (3) articles in other languages.

Data Extraction

Each qualifying paper was independently evaluated by two reviewers. Each article was analyzed for the number of patients, their age, procedure modality, and incidence of the pre decided complications. Further discussion or consultation with the author and a third party was used to resolve conflicts. The study's quality was assessed using the modified Jadad score. In the end, According to PRISMA, a total of 10 RCTs pertaining to use of SMI with a total of 1,847 patients, 7 RCTs pertaining to Radionuclide Scanning with 1,152 patients, 8 RCTs pertaining to CD with 4,480 patients were selected for further analysis.

Assessment of Study Quality

Using the QualSyst tool, two writers independently assessed the caliber of each included study. This test consists of 10 questions, each with a score between 0 and 2, with 20 being the maximum possible overall score. Two authors rated each article independently based on the above criteria. The interobserver agreement for study selection was determined using the weighted Cohen's kappa (K) coefficient. For deciding the bias risk for RCTs, we also employed the Cochrane tool. No assumptions were made about any missing or unclear information. there was no funding involved in collecting or reviewing data.

Statistical Analysis

The statistical software packages RevMan (Review Manager, version 5.3), SPSS (Statistical Package for the Social Sciences, version 20), Google Sheets, and Excel in Stata 14 were used to perform the statistical analyses. The data was obtained and entered into analytic software [21]. Fixed- or random-effects models were used to estimate Sensitivity, Specificity, positive predictive value (PPV), diagnostic odds ratios (DOR), and relative risk (RR) with 95 percent confidence intervals to examine critical clinical outcomes (CIs). Diagnosis accuracy and younden index were calculated for each result. Individual study sensitivity and specificity were plotted on Forest plots and in the receiver operating characteristic (ROC) curve. The forest plot and Fagan's Nomogram were used to illustrate the sensitivity and specificity of different papers.(8)

Bias Study

The risk of bias was evaluated by using QUADAS-2 analysis. This tool includes 4 domains as Patient selection, Index test, Reference standard, Flow of the patients, and Timing of the Index tests.

Radionuclide:

	Patient Selection	Index Test	Reference Standard	Flow and Timing	Patient Selection	Index Test	Reference Standard
Basharat 2011(9)	low	low	low	high	low	low	low
Deandreis 2012(10)	low	low	low	low	low	low	unclear

Lin 2009(11)	low	low	low	unclear	low	low	low
Lumachi 2004(12)	low	low	unclear	low	low	unclear	low
Muñoz Pérez 2013(13)	low	unclear	low	low	low	low	low
Piccardo 2016(14)	low	low	low	low	low	low	high
Riazi 2014(15)	low	unclear	low	low	low	low	low

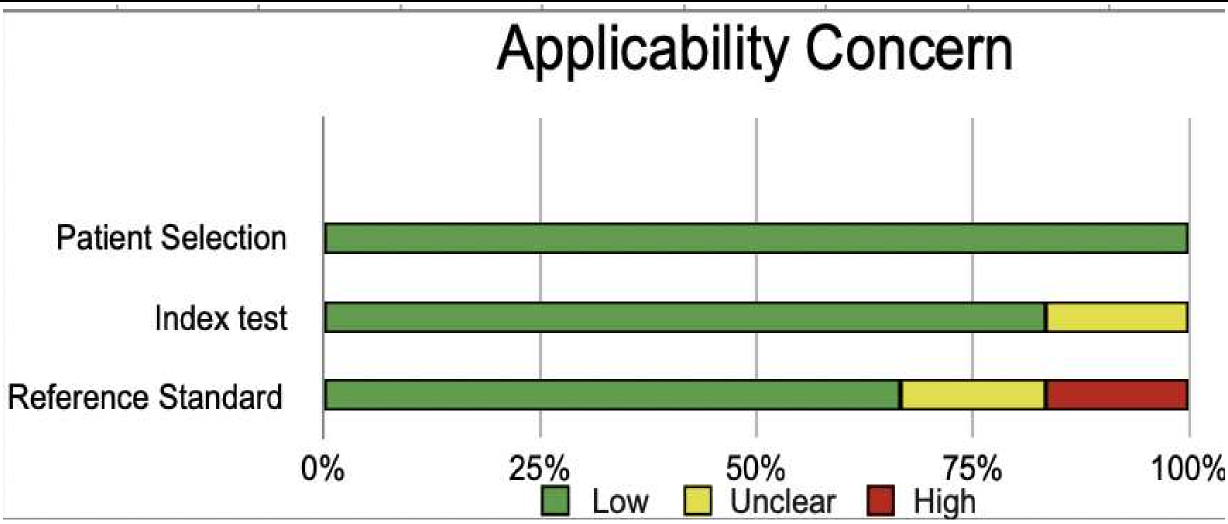

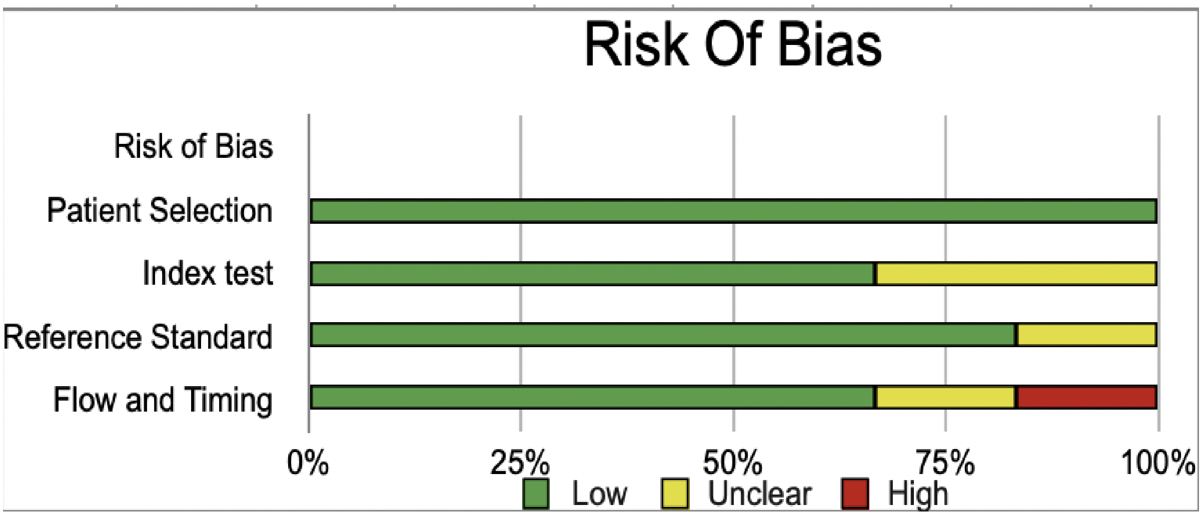

SMI:

	Patient Selection	Index Test	Reference Standard	Flow and Timing	Patient Selection	Index Test	Reference Standard
Chen 2017(16)	low	low	high	unclear	low	low	low
Diao 2016(17)	low	unclear	low	low	low	low	low
He 2020(18)	low	high	low	low	low	low	unclear
Li 2017(19)	low	low	unclear	low	low	unclear	high
Li 2020(20)	low	unclear	low	low	low	low	low

Preprints.org (www.preprints.org) | NOT PEER-REVIEWED | Posted: 21 December 2023 doi:10.20944/preprints202312.1669.v1

Pei 2019(21)	low	low	unclear	low	high	low	low
Wang 2021(22)	high	low	low	low	low	high	low
Yang 2017(23)	unclear	low	low	unclear	low	low	low
Zhao 2019(24)	low	low	unclear	low	low	high	low
Zhu 2018(25)	low	low	low	unclear	low	low	low

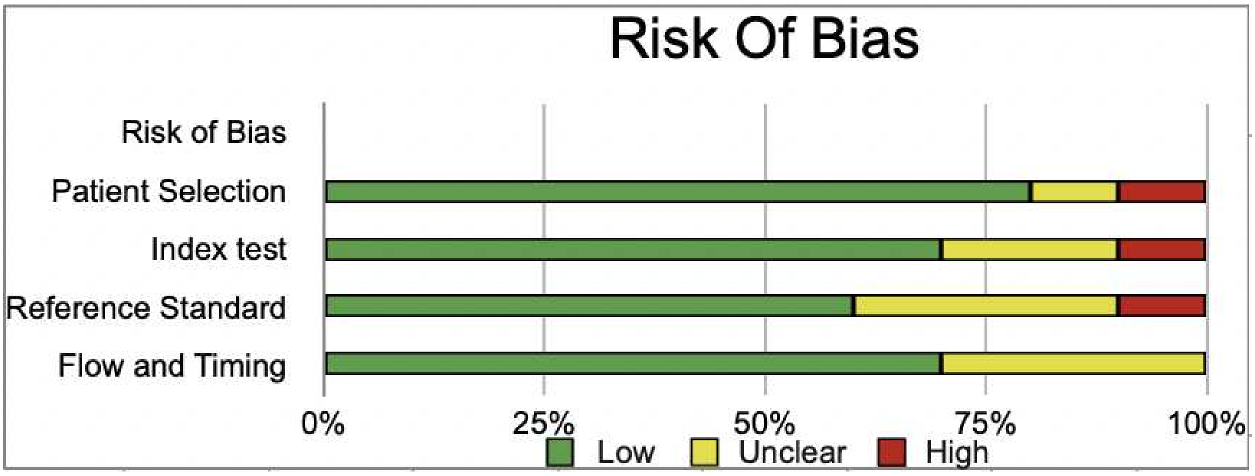

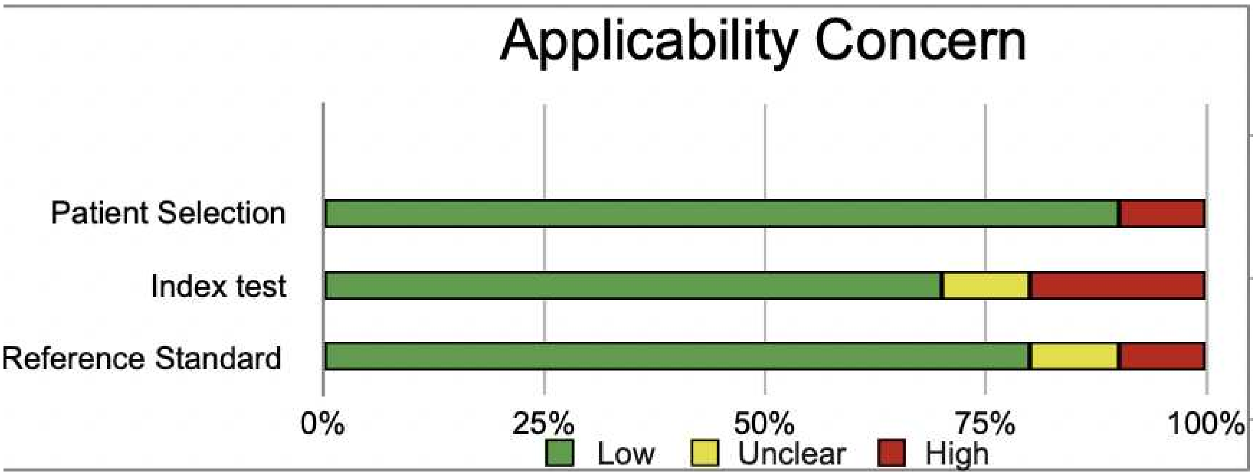

Color doppler:

	Patient Selection	Index Test	Reference Standard	Flow and Timing	Patient Selection	Index Test	Reference Standard
Bozbora 2002(26)	low	unclear	low	low	low	low	low
Gannon 2018(27)	low	low	unclear	low	low	low	unclear
Gul 2009(28)	low	low	low	low	low	low	low
Li 2016(29)	low	low	unclear	low	low	unclear	low
Lin 2009(30)	high	unclear	low	low	low	low	low
Ma 2014(31)	low	low	unclear	low	low	low	high
Palaniappan 2016(32)	unclear	low	low	low	low	low	low

Preprints.org (www.preprints.org) | NOT PEER-REVIEWED | Posted: 21 December 2023 doi:10.20944/preprints202312.1669.v1

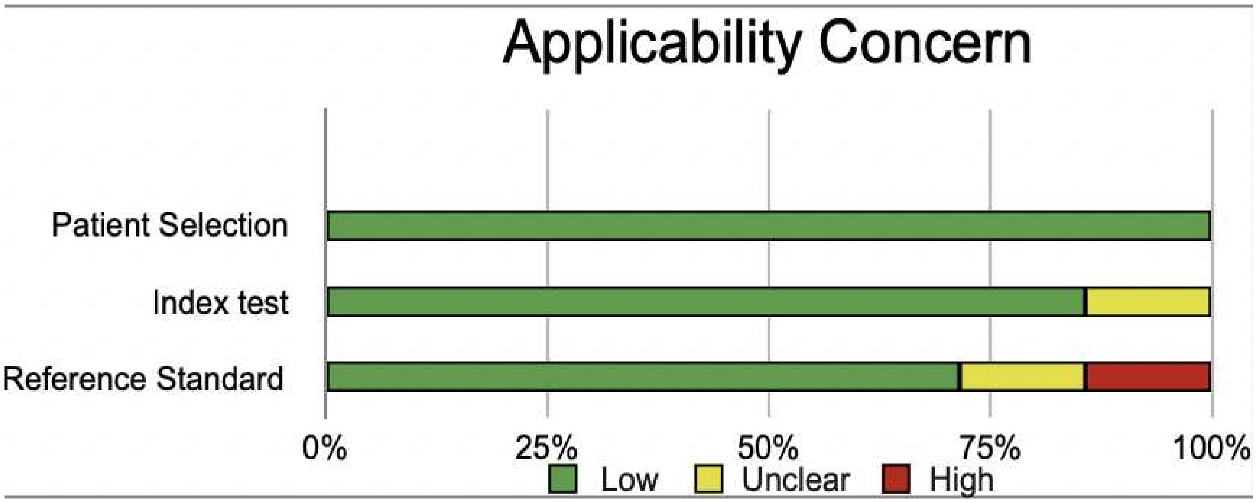

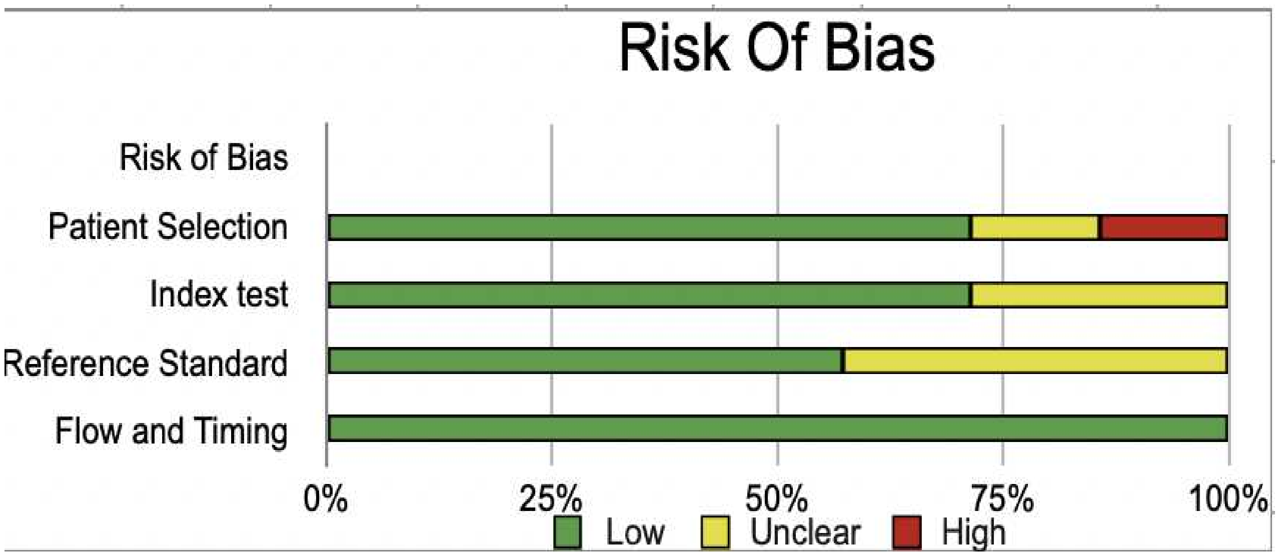

Result:

Table 1. Radionuclide Scanning.

Author Name and Year	**R Basharat 2011(9)**	**D Deandreis 2012(10)**	**Jia-Hau Lin 2009(11)**	**F Lumachi 2004(12)**	**Muñoz Pérez 2013(13)**	**A Piccardo 2016(14)**	**A Riazi 2014(15)**
Country	Pakistan	France	Taiwan	Italy	Spain	Italy/ Switzerland	Iran
Language	English	English	English	English	English	English	English
Period of Study	6 months	Nov 2006 to Oct 2009	Jan 1993 to Dec 2006	2002 to 2003	Jan 2009 to Apr 2012	Not Specified	May 2011 to Apr 2013
Modality Applied	Radionuclide Screening	Radionuclide Screening	Radionuclide Screening	Radionuclide Screening	Radionuclide Screening	Radionuclide Screening	Radionuclide Screening
Radionuclide used	Iodine123/ Tc99m pertechnetate	(18)F-fluorodeoxyglucose	99mTc-pertechnetate	99mTc-pertechnetate	(18)F-fluorodeoxyglucose	(18)F-fluorodeoxyglucose	Tc-99m Methoxyisobutylisonitrile
Type of Study	Cross sectional study	Prospective Study	Retrospective Study	Retrospective Study	Prospective Study	Not specified	Prospective Study

 doi:10.20944/preprints202312.1669.v1

Reference Standard	Postoperative histopathology	Postoperative histopathology	Postoperative histopathology	Postoperative histopathology	Postoperative histopathology	Postoperative histopathology	Postoperative histopathology
True Positive (TP)	36	21	195	315	12	32	20
False Negetive (FN)	9	2	66	85	1	8	0
True Negetive (TN)	4	13	48	92	17	10	9
False Positive (FP)	1	8	17	4	16	37	74
Total	50	44	326	496	46	87	103

Table 2. SMI.

Author	**X Chen 2017(16)**	**X Diao 2016(17)**	**He 2020(18)**	**Y H Li 2017(19)**	**Li 2020(20)**	**Shufang Pei 2019(21)**	**Wang 2021(22)**	**GX Yang 2017(23)**	**Yongfeng Zhao 2019(24)**	**YI-Cheng Zhu 2018(25)**
Country	China	China	China	China	China	China	China	China	China	China
Language	Chinese	English/ Chinese	Chinese	Chinese	Chinese	English	Chinese	Chinese	English/ Chinese	English
Sample Age (years)	45.2 ± 18.5	44.8 ± 17.6	43.9 ± 10.2	39.0 ± 16.5	19 to 68	Not specified	46.6 ± 18.6	49.4 ± 12.5	Not specified	49.6 ± 13.2
Modality Applied	Superb microvascular imaging (SMI)	Superb microvascular imaging (SMI)	Superb microvascular imaging (SMI)	Superb microvascular imaging (SMI)	Superb microvascular imaging (SMI)	Superb microvascular imaging (SMI)	Superb microvascular imaging (SMI)	Superb microvascular imaging (SMI)	Superb microvascular imaging (SMI)	Superb microvascular imaging (SMI)
Instrument used	Toshiba Aplio-500	Toshiba Aplio-500	Toshiba Aplio-500	Toshiba Aplio-500	Toshiba Aplio-500	Toshiba Aplio-500	Toshiba Aplio-500	Toshiba Aplio-500	Toshiba Aplio-500	Toshiba Aplio-500
Reference Standard	Histologically confirmed	Histologically confirmed	Histologically confirmed	Histologically confirmed	Histologically confirmed	Histologically confirmed	Histologically confirmed	Histologically confirmed	Histologically confirmed	Histologically confirmed
True Positive (TP)	48	24	30	58	36	92	306	33	105	25
False Negetive (FN)	10	3	11	15	9	26	48	7	34	4
True Negetive (TN)	99	39	22	158	44	73	134	48	136	40
False Positive (FP)	6	2	6	23	11	5	37	12	21	7
Total	163	68	69	254	100	196	525	100	296	76

Table 3. Color Doppler Ultrasound.

Author	**A Bozbora 2002(26)**	**A W Gannon 2018(27)**	**Kamile Gul 2009(28)**	**Ru-Qiang Li 2016(29)**	**Jia-Hau Lin 2009(30)**	**Jiao-jiao Ma 2014(31)**	**M K Palaniappan 2016(32)**	**F Stacul 2007(33)**
Country	Turkey	USA	Turkey	China	Taiwan	China	India	Italy
Language	English	English	English	English	English	English	English	English/ Italian
Period of Study	Not Specified	Jan 2009 to Mar 2013	2005 to 2008	Mar 2011 to July 2014	Jan 1993 to Dec 2006	Not Specified	Mar 2013 to Apr 2015	Jan 2004 to June 2005
Modality Applied	Color Doppler Ultrasound	Color Doppler Ultrasound	Color Doppler Ultrasound	Color Doppler Ultrasound	Color Doppler Ultrasound	Color Doppler Ultrasound	Color Doppler Ultrasound	Color Doppler Ultrasound
Type of Study	Not Specified	Retrospective cohort study	Retrospective cohort study	Retrospective cohort study	Retrospective cohort study	Not Specified	Prospective case control study	Prospective study
Reference Standard	FNAB	FNAB	FNAB	FNAB	FNAB	FNAB	FNAB	FNAB
True Positive (TP)	14	35	141	338	41	84	36	110
False Negetive (FN)	7	24	17	86	40	10	7	129
True Negetive (TN)	60	85	1,900	241	281	73	131	307
False Positive (FP)	0	8	24	97	16	5	20	113
Total	81	152	2082	762	378	172	194	659

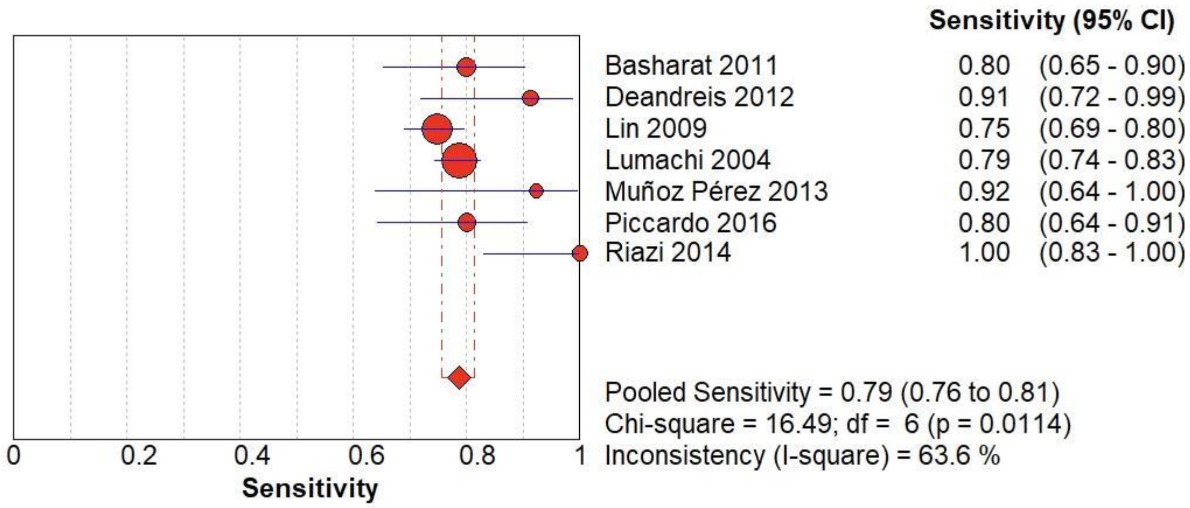

Preprints.org (www.preprints.org) | NOT PEER-REVIEWED | Posted: 21 December 2023 doi:10.20944/preprints202312.1669.v1

Figure 3. (**A**) The forest chart summary for pooled sensitivity values of Radionuclide Scanning for thyroid nodules.

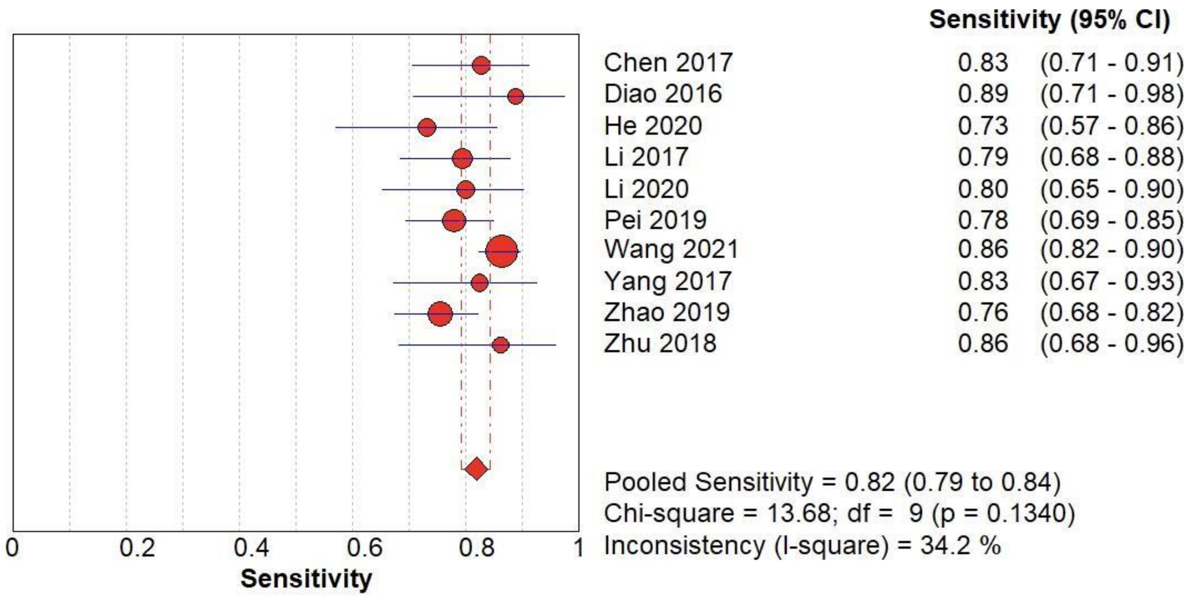

Figure 3. (**B**) The forest chart summary for pooled sensitivity values of SMI for thyroid nodules.

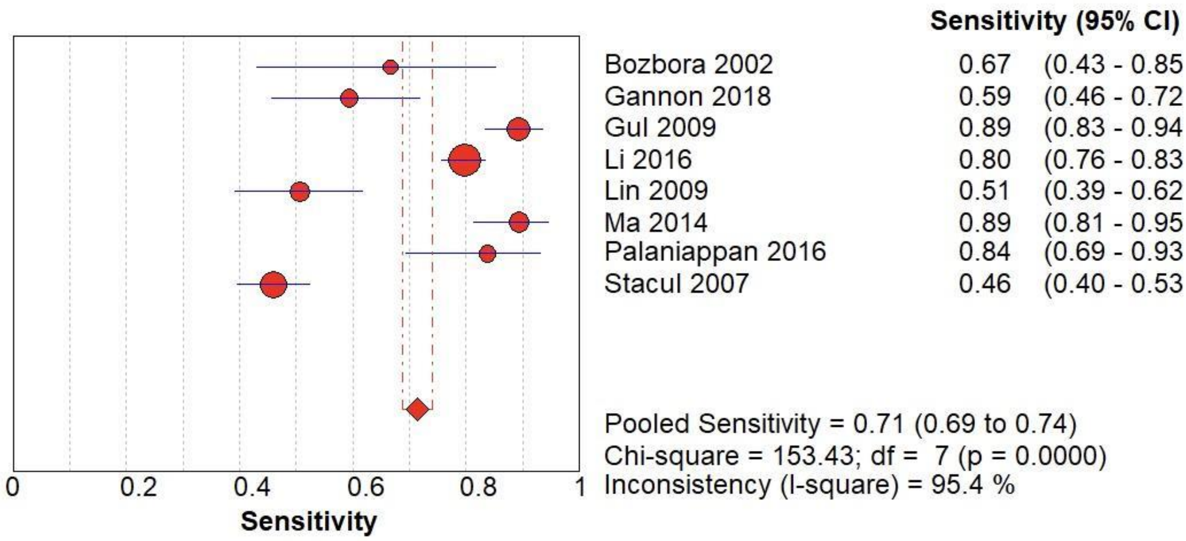

Figure 3. (**C**) The forest chart summary for pooled sensitivity values of CD for thyroid nodules.

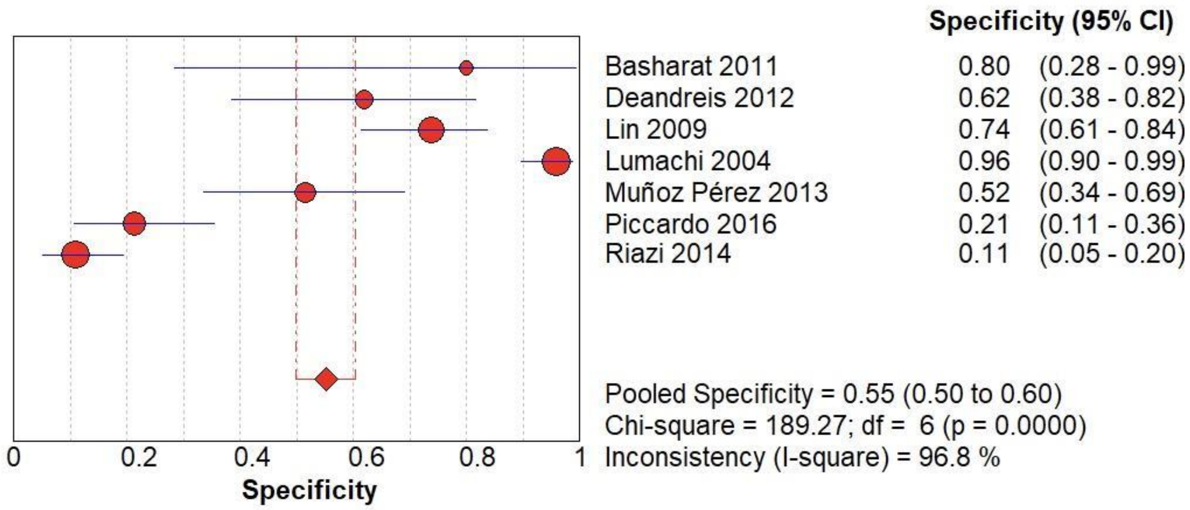

Figure 4. (**A**) The forest chart summary for pooled specificity values of Radionuclide Scanning for thyroid nodules.

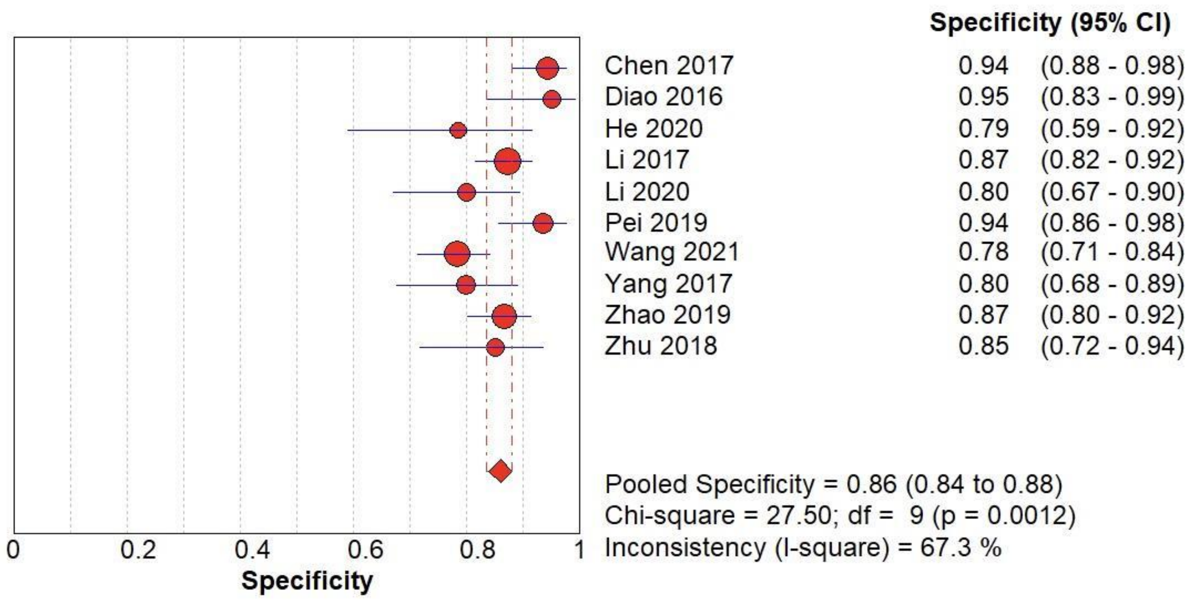

Figure 4. (**B**) The forest chart summary for pooled specificity values of SMI for thyroid nodules.

Preprints.org (www.preprints.org) | NOT PEER-REVIEWED | Posted: 21 December 2023 doi:10.20944/preprints202312.1669.v1

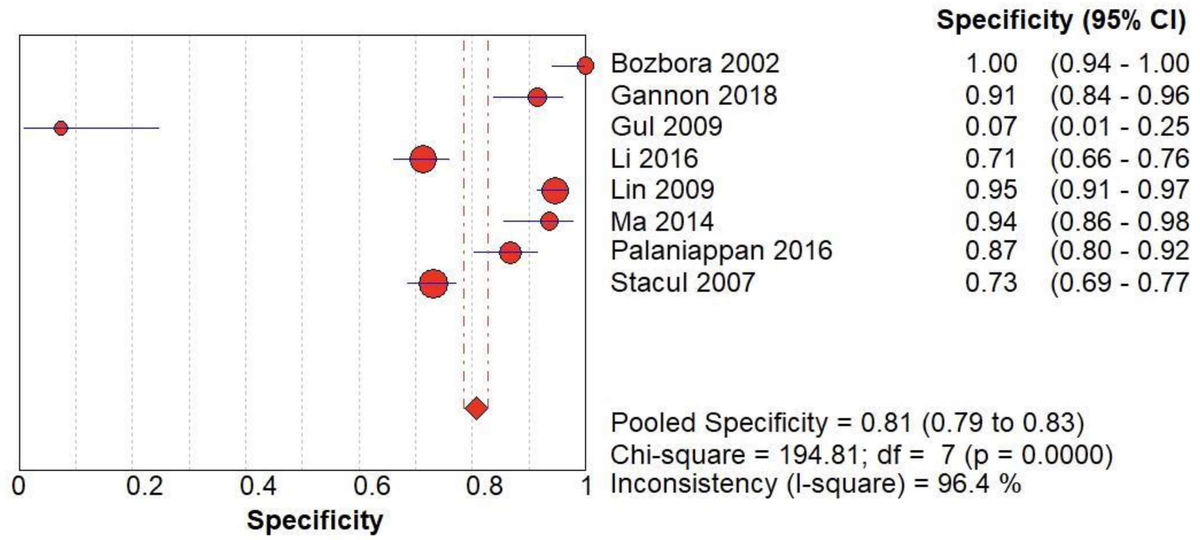

Figure 4. (**C**) The forest chart summary for pooled specificity values of CD for thyroid nodules.

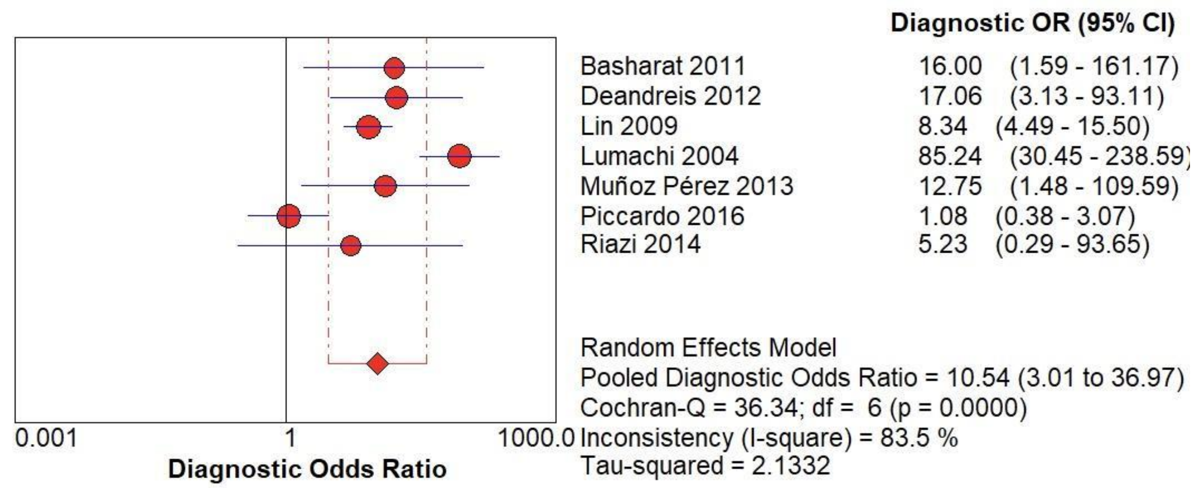

Figure 5. (**A**) The forest chart summary for pooled Diagnostic Odd's Ratio of Radionuclide Scanning for thyroid nodules.

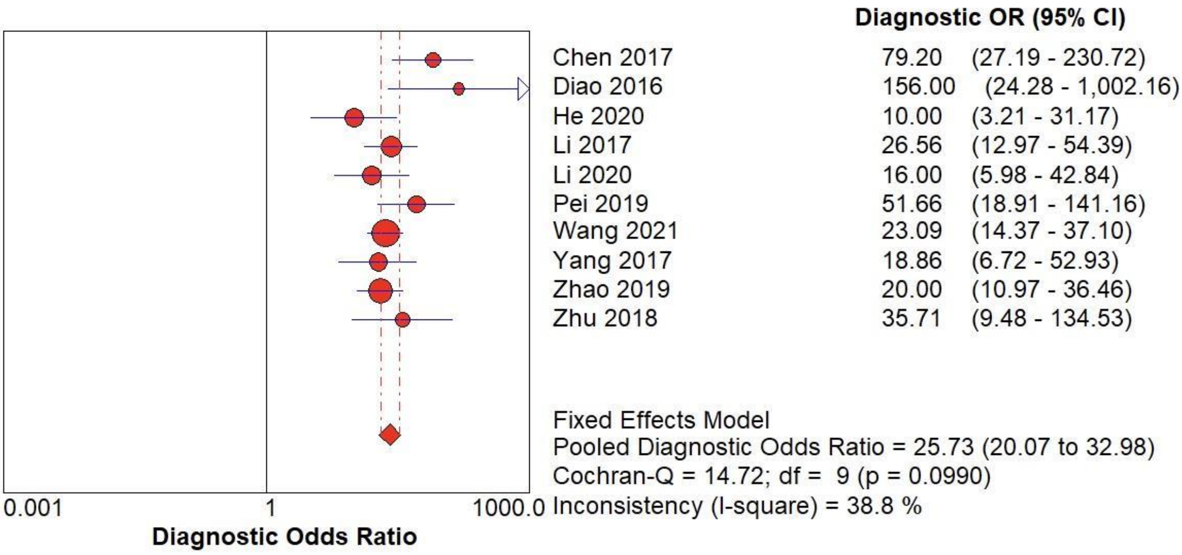

Figure 5. (**B**) The forest chart summary for pooled Diagnostic Odd's Ratio of SMI for thyroid nodules.

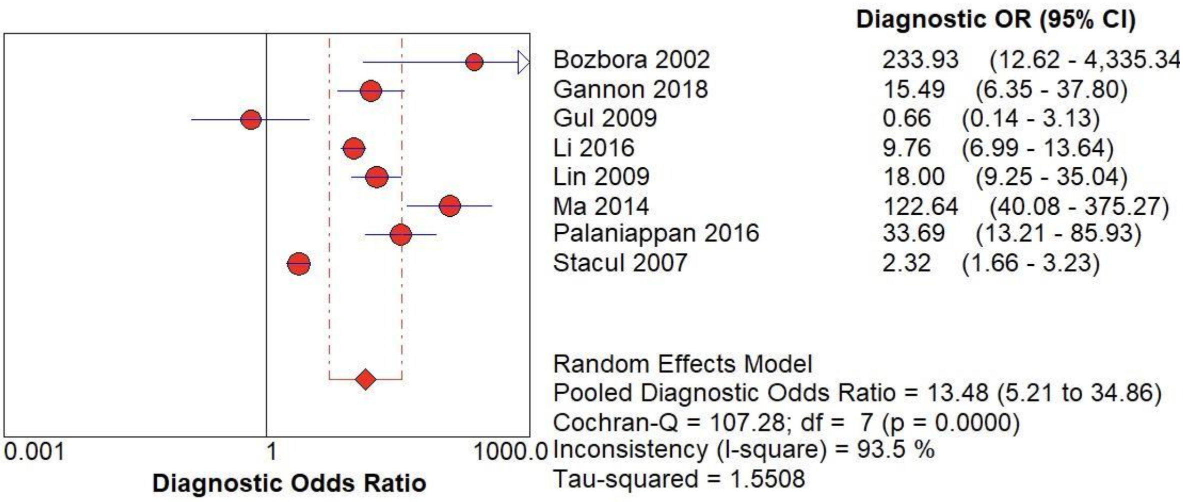

Figure 5. (**C**) The forest chart summary for pooled Diagnostic Odd's Ratio of CD for thyroid nodules.

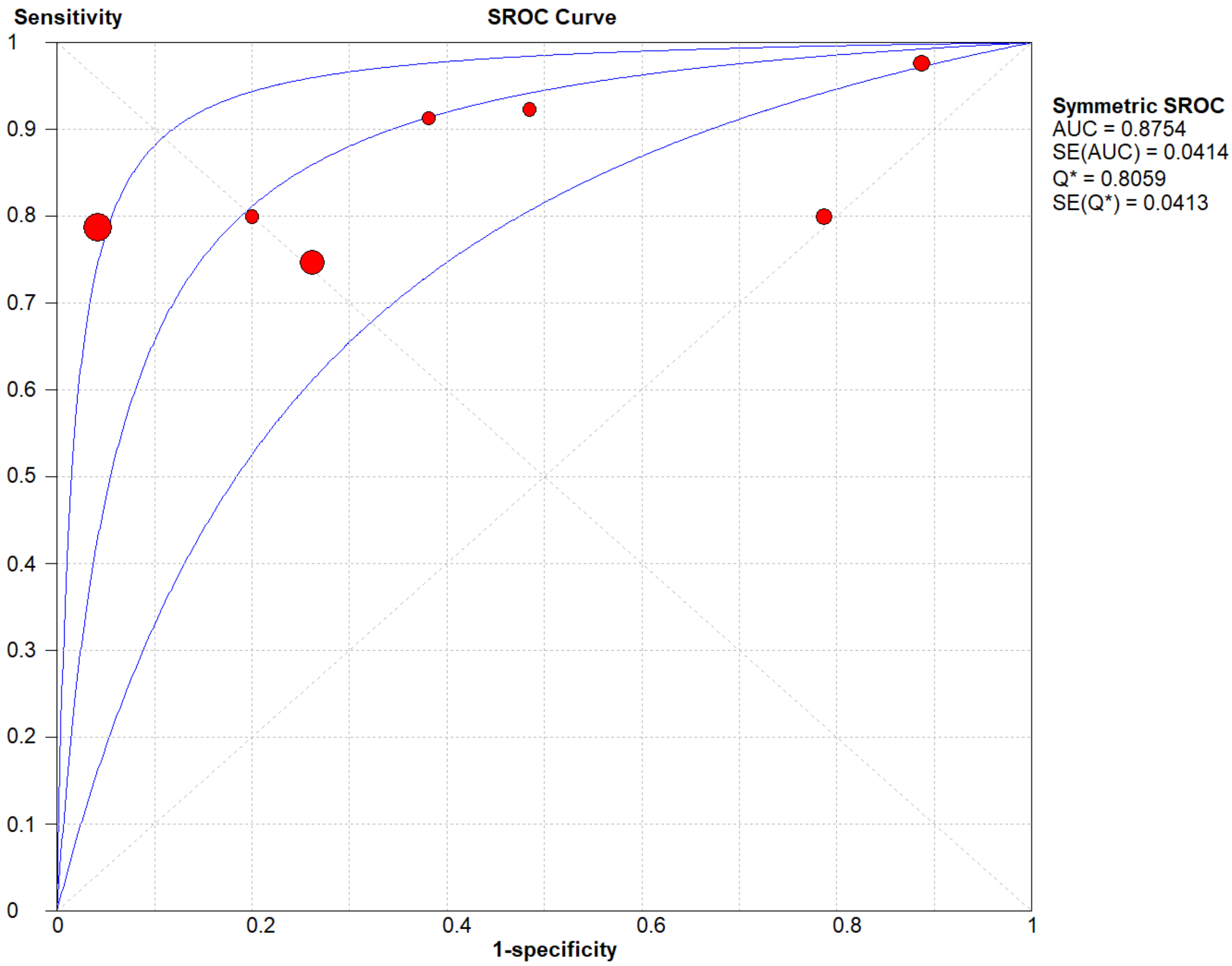

Figure 6. (**A**) The SROC plot summary for Radionuclide Scanning for thyroid nodules.

Preprints.org (www.preprints.org) | NOT PEER-REVIEWED | Posted: 21 December 2023 doi:10.20944/preprints202312.1669.v1

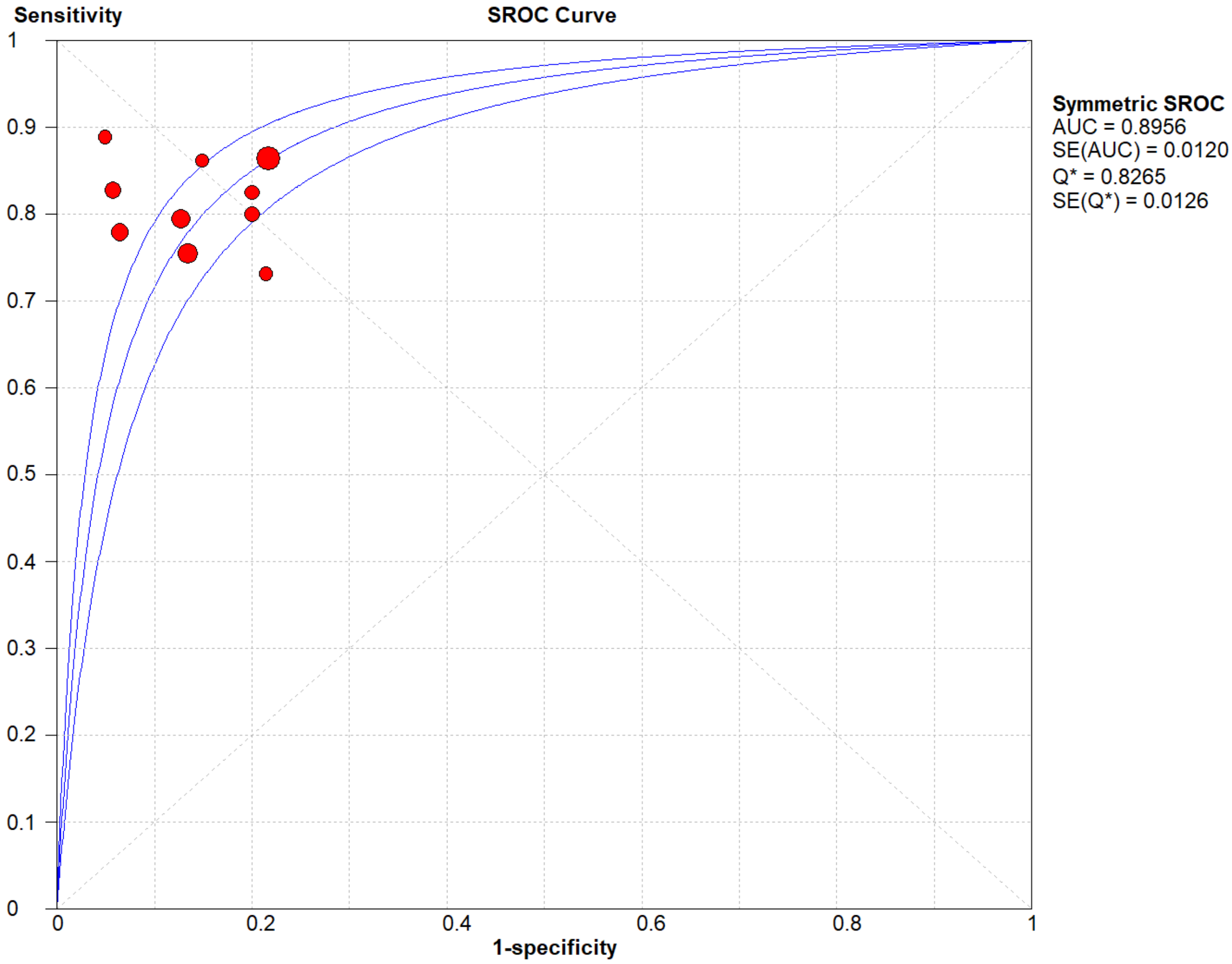

Figure 6. (**B**) The SROC plot summary for SMI for thyroid nodules.

Preprints.org (www.preprints.org) | NOT PEER-REVIEWED | Posted: 21 December 2023 doi:10.20944/preprints202312.1669.v1

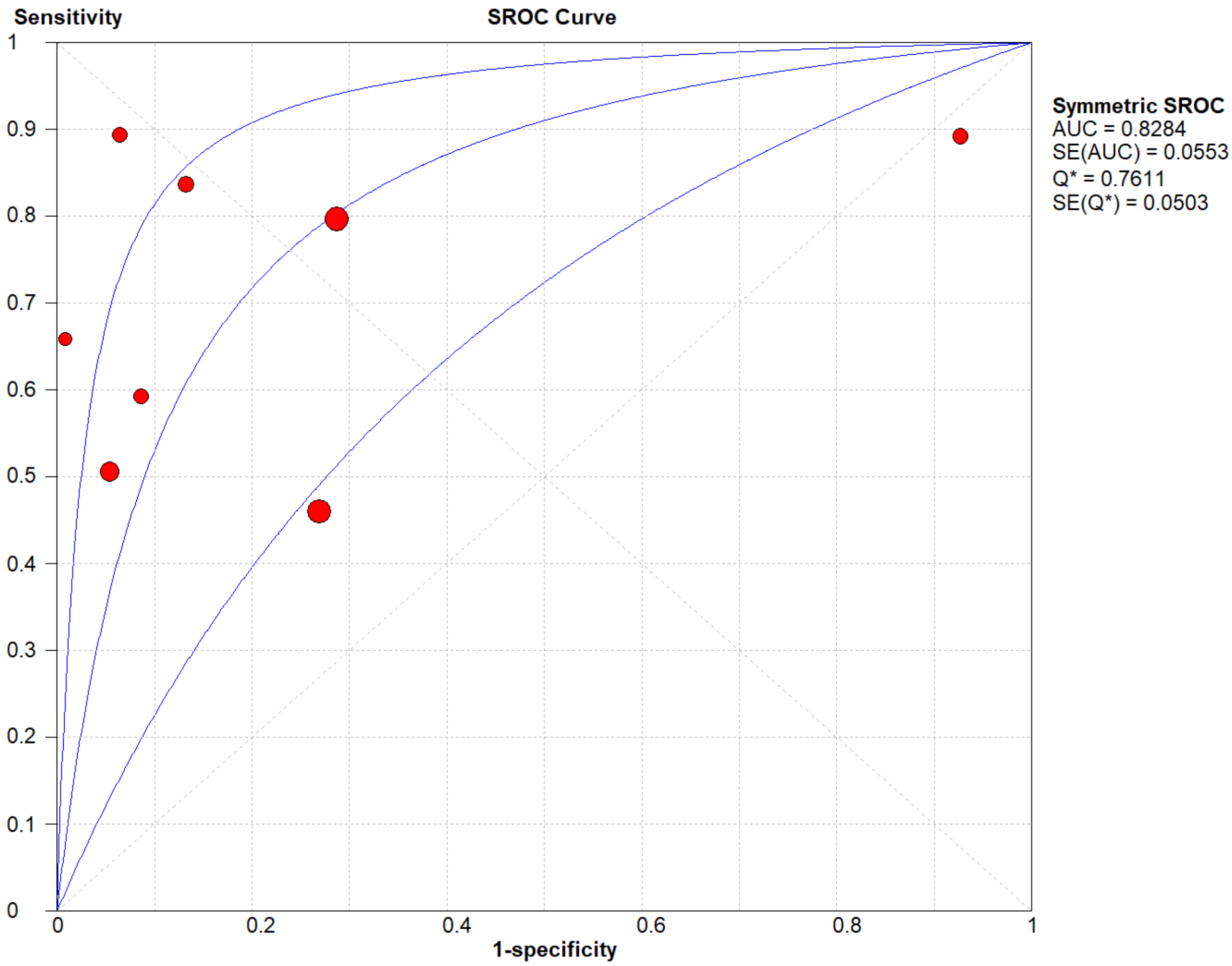

Figure 6. (**C**) The SROC plot summary for CD for thyroid nodules.

Figure 7. (**A**) Funnel Plot for Radionuclide Scanning for thyroid nodules.

Figure 7. (**B**) Funnel Plot for SMI for thyroid nodules.

Figure 7. (**C**) Funnel Plot for CD for thyroid nodules.

Radionuclide Scanning vs Histopathology for Thyroid Nodules

Here, Table 1 describes all the descriptions of papers used for Radionuclide Scanning vs Histopathology analysis. All the results described above, in the forest chart (Figures 3A and 4A), the comparison of the sensitivity and specificity of different papers can be observed. The same is illustrated in the SROC curve. (Figure 6A). A total of 7 RCTs with 1,152 patients were selected for the study, out of which 1 study showed sensitivity at or above 95%, and 1 study showed specificity at or above 95%. There were no studies that showed both sensitivity and specificity, to be at or over 95%. The value of True Positive (TP) was 631, that of True Negative (TN) was 193, that of False Positive (FP) was 157, and that of False Negative (FN) was 171. The pooled sensitivity of Radionuclide Scanning is 0.79, with a CI of 95% in a range of 0.76 to 0.81. The specificity of Radionuclide Scanning is 0.55, with a CI of 95% in a range of 0.50 to 0.60.

The summary of the ROC curve is described in Figure 6A. It shows that the area under the curve for Radionuclide Scanning was 0.8754 and the overall diagnostic odds ratio (DOR) (4A) was 10.54.

 doi:10.20944/preprints202312.1669.v1

SMI vs Histopathology for Thyroid Nodules

Here, Table 2 describes all the descriptions of papers used for SMI vs Histopathology analysis. All the results described above, in the forest chart (Figures 3B and 4B), the comparison of the sensitivity and specificity of different papers can be observed. The same is illustrated in the SROC curve. (Figure 6B). A total of 10 RCTs with 1,847 patients were selected for the study, out of which no study showed sensitivity at or above 95%, and 1 study showed specificity at or above 95%. There were no studies that showed both sensitivity and specificity, to be at or over 95%. The value of True Positive (TP) was 757, that of True Negative (TN) was 793, that of False Positive (FP) was 130, and that of False Negative (FN) was 167. The pooled sensitivity of SMI is 0.82, with a CI of 95% in a range of 0.79 to 0.84. The specificity of SMI is 0.86, with a CI of 95% in a range of 0.84 to 0.88.

The summary of the ROC curve is described in figure 6B. It shows that the area under the curve for SMI was 0.8956 and the overall diagnostic odds ratio (DOR) (4B) was 25.73.

CD vs Histopathology for Thyroid Nodules

Here, Table 3 describes all the descriptions of papers used for CD vs Histopathology analysis. All the results described above, in the forest chart (Figures 3C and 4C), the comparison of the sensitivity and specificity of different papers can be observed. The same is illustrated in the SROC curve. (Figure 6C). A total of 8 RCTs with 4,480 patients were selected for the study, out of which no study showed sensitivity at or above 95%, and 1 study showed specificity at or above 95%. There were no studies that showed both sensitivity and specificity, to be at or over 95%. The value of True Positive (TP) was 799, that of True Negative (TN) was 3078, that of False Positive (FP) was 283, and that of False Negative (FN) was 320. The pooled sensitivity of CD is 0.71, with a CI of 95% in a range of 0.69 to 0.74. The specificity of CD is 0.81, with a CI of 95% in a range of 0.79 to 0.83.

The summary of the ROC curve is described in figure 6C. It shows that the area under the curve for CD was 0.8284 and the overall diagnostic odds ratio (DOR) (4C) was 13.48.

Preprints.org (www.preprints.org) | NOT PEER-REVIEWED | Posted: 21 December 2023 doi:10.20944/preprints202312.1669.v1

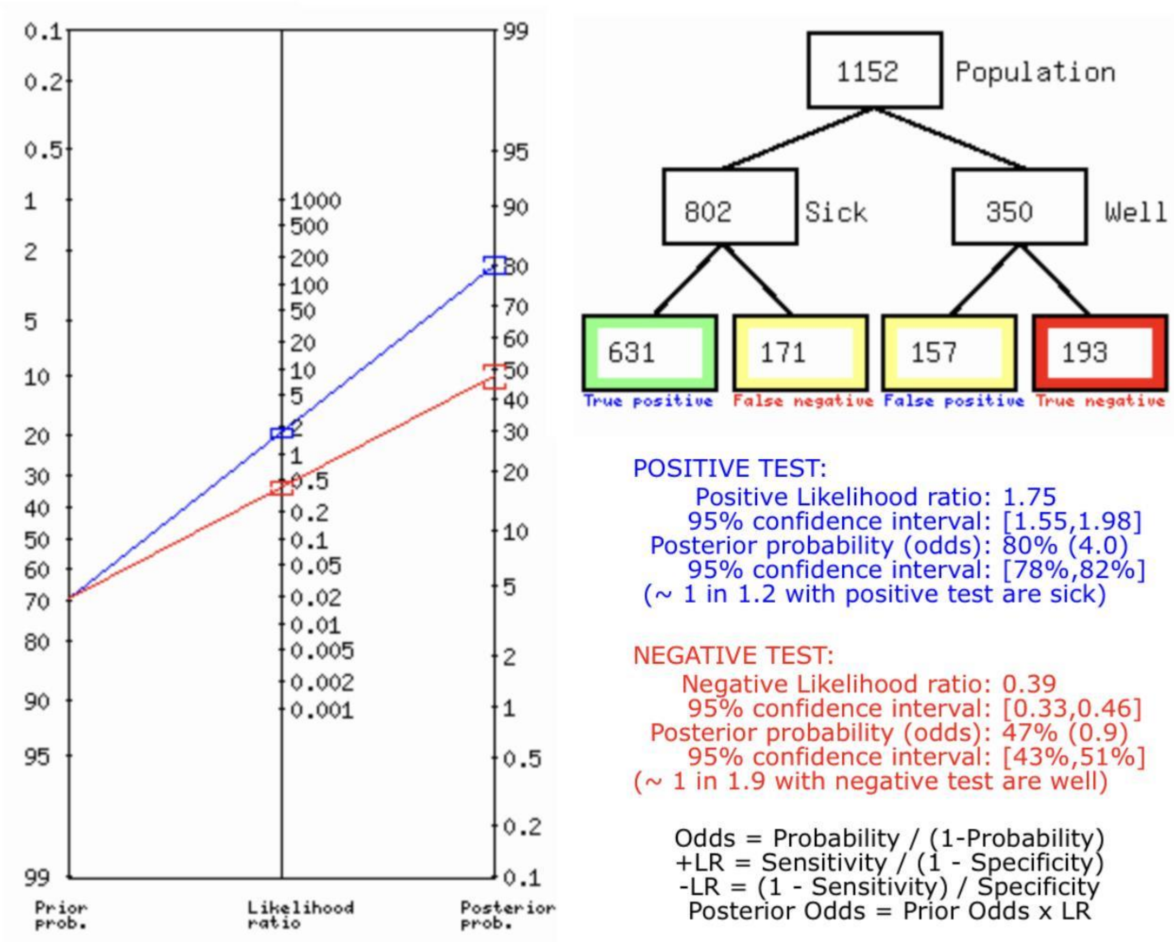

Figure 8. (**A**) Fagan's Analysis for RADIONUCLIDE SCANNING vs HISTOPATHOLOGY for thyroid nodules.

Figure 8A describes the summary of Fagan plot analysis for all the studies considered for Radionuclide Scanning vs Histopathology for diagnosis of thyroid nodules, showing a prior probability of 70% (2.3); a Positive Likelihood Ratio of 1.75; a probability of post-test 80% (4.0); a Negative Likelihood Ratio of 0.39, and a probability of post-test 47% (0.9).

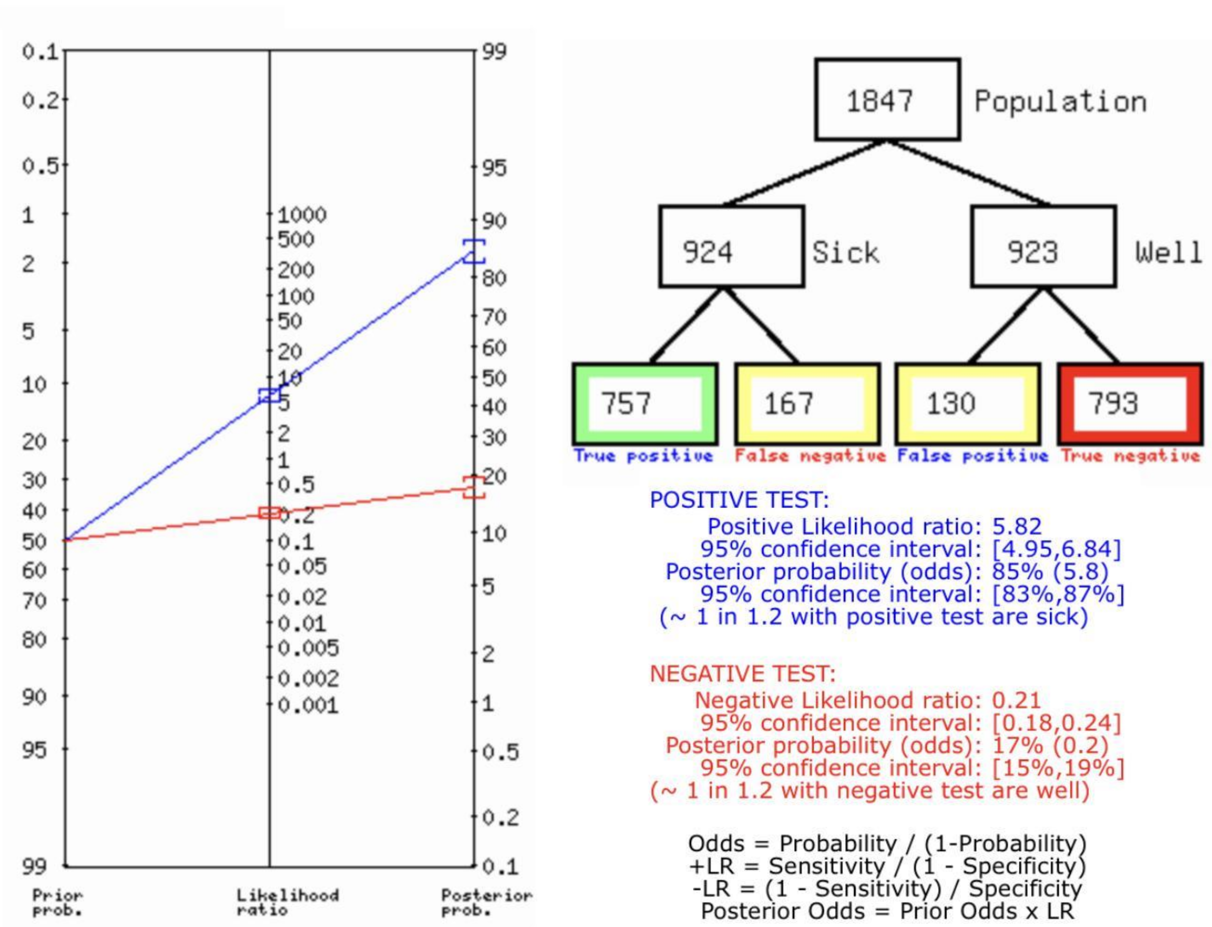

Figure 8. (B) Fagan's Analysis for SMI vs HISTOPATHOLOGY for thyroid nodules.

Figure 8B describes the summary of Fagan plot analysis for all the studies considered for SMI vs Histopathology for diagnosis of thyroid nodules, showing a prior probability of 50% (1.0); a Positive Likelihood Ratio of 5.82; a probability of post-test 85% (5.8); a Negative Likelihood Ratio of 0.21, and a probability of post-test 17% (0.2).

Preprints.org (www.preprints.org) | NOT PEER-REVIEWED | Posted: 21 December 2023 doi:10.20944/preprints202312.1669.v1

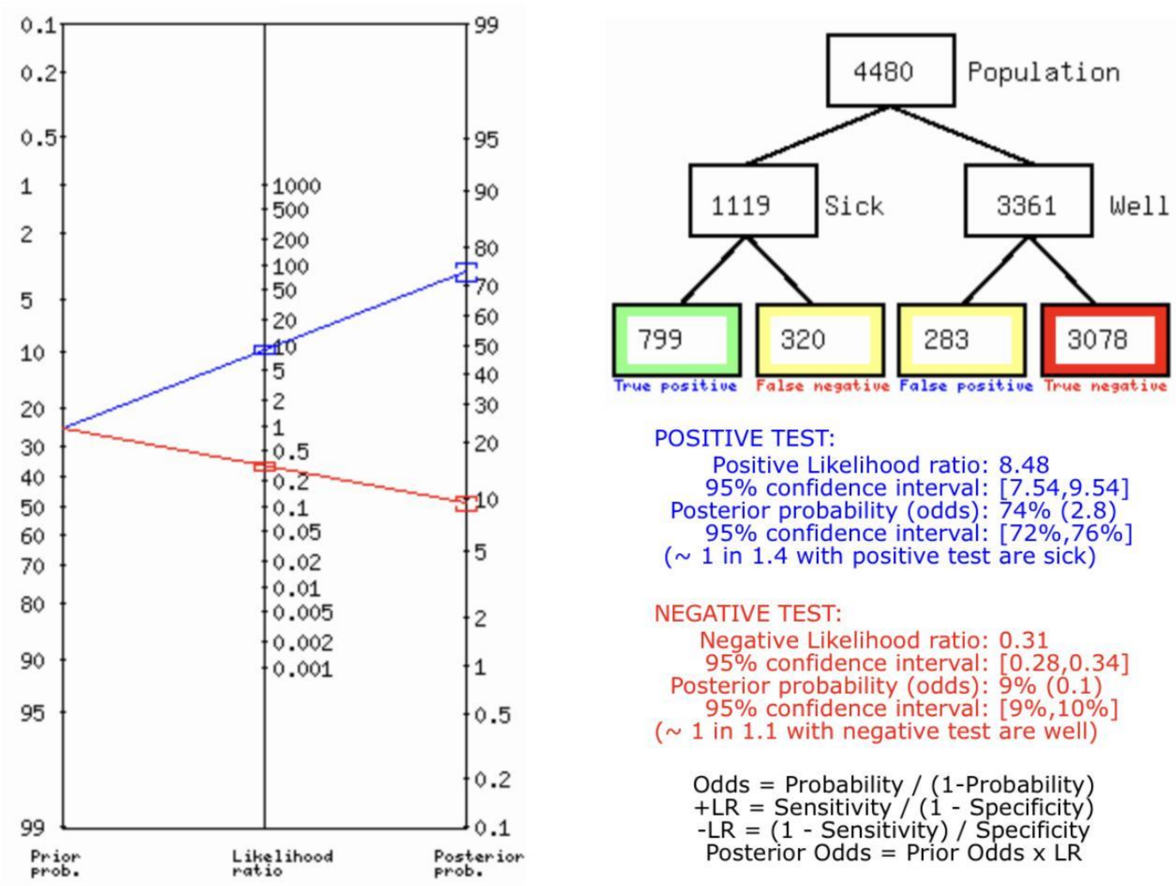

Figure 8. (**C**) Fagan's Analysis for CD vs HISTOPATHOLOGY for thyroid nodules.

Figure 8C describes the summary of Fagan plot analysis for all the studies considered for CD vs Histopathology for diagnosis of thyroid nodules, showing a prior probability of 25% (0.3); a Positive Likelihood Ratio of 8.48; a probability of post-test 74% (2.8); a Negative Likelihood Ratio of 0.31, and a probability of post-test 9% (0.1).

Table 4. Network analysis and ANOVA test.

	SMI	**Radionuclide Imaging**	**Colour Doppler**	**SPECIFICITY**
		0.0082	0.9468	SMI
SMI			**0.0039**	Radionuclide Imaging
Radionuclide Imaging	0.7586			Colour doppler
Colour doppler	0.1613	**0.0402**		
SENSITIVITY	SMI	Radionuclide Imaging	Colour doppler	

The ANOVA test for Sensitivity had a p-value of 0.48892 at a significance level at p<0.05 and an f-ratio of 3.47282. For Specificity, the p-value was at 0.003315 with the same significance level and f-ratio at 7.48409.

While drawing the pairwise comparison with the help of p-value at the significance level of p<0.05, For Sensitivity, only a statistically significant difference diagnostically was found between Colour Doppler and Radionuclide imaging but for Specificity, a statistically significant difference was found between SMI and radionuclide imaging, and Radionuclide imaging & Colour Doppler. All other pairwise comparisons were statistically insignificant in both sensitivity and specificity.

Preprints.org (www.preprints.org) | NOT PEER-REVIEWED | Posted: 21 December 2023 doi:10.20944/preprints202312.1669.v1

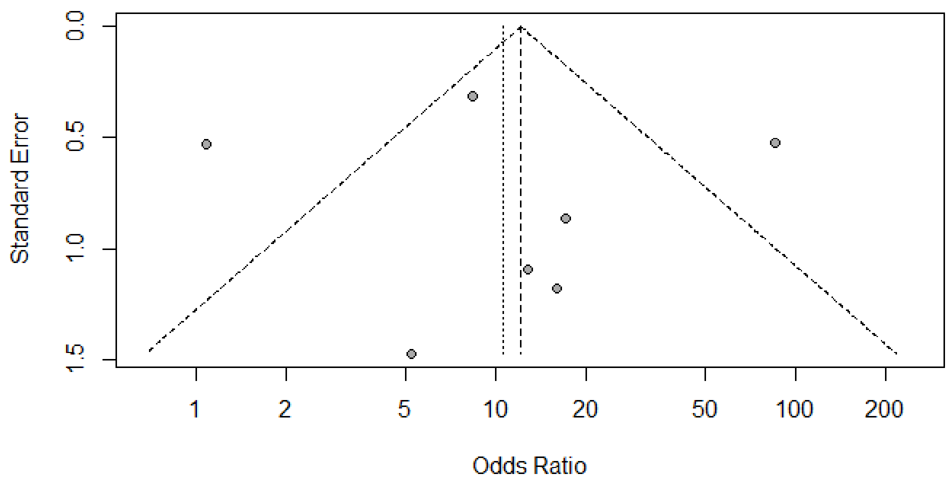

Figure 9. (**A**) Deek's Funnel Plot for RADIONUCLIDE SCANNING vs HISTOPATHOLOGY for thyroid nodules.

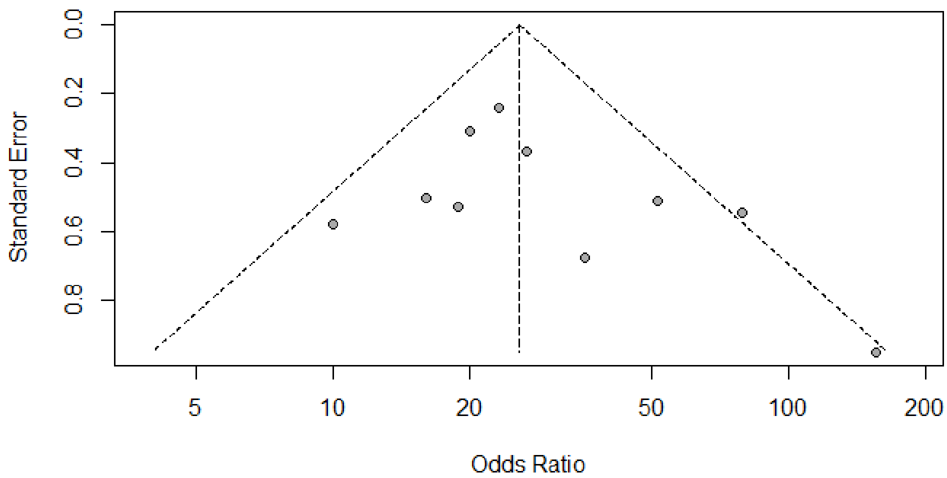

Figure 9. (**B**) Deek's Funnel Plot for SMI vs HISTOPATHOLOGY for thyroid nodules.

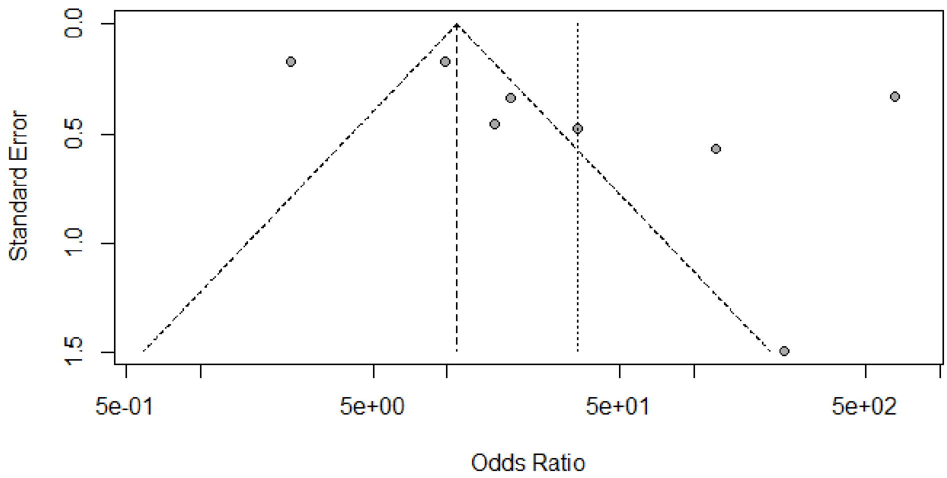

Figure 9. (**C**) Deek's Funnel Plot for CD vs HISTOPATHOLOGY for thyroid nodules.

Discussion

Thyroid nodules have been identified in almost 65% of the general population. This underscores their prevalence as a widespread condition. It is important to note that a large portion of these nodules are non-cancerous, and can be effectively managed through vigilant monitoring protocols. The primary objective of initial screening and ongoing tracking of thyroid nodules is to enhance management of the most concerning thyroid malignancies.(34)

In this meta-analysis, we have compared multiple blood flow dependent imaging techniques used to detect thyroid nodules, both benign and malignant. Our analysis is based on all eligible diagnostic studies and scientific papers based on this subject.

Our results show a pooled sensitivity of 0.819 or 81.9% (0.79-0.84) and specificity of 0.86 or 86% (0.84-0.88) for SMI, and PPV of 0.853. Our results for colour doppler show a sensitivity of 0.71 or 71% (0.69-0.74), specificity of 0.81 or 81% (0.79-0.83) and PPV of 0.738. This paper also shows pooled sensitivity of 0.79 (0.76-0.81) and pooled specificity of 0.55 (0.50-0.60) for radionuclide studies.

Conventional sonographic techniques are used to differentiate between benign and malignant thyroid nodules by showing echogenicity, margins, presence of microcalcifications, as well as vascular flow, which is the choice of first-screen by doctors. Recent advances in technology have had the effect of increasing the accuracy of ultrasound in the diagnosis of thyroid nodules.(35)

Determining the characteristics as well as the presence of vascular flow is an essential part of sonography interrogation. However, due to the nature of small vessels and low velocities, it is not always possible to depict conventional color and power Doppler ultrasound. This is a challenging aspect of forming a differential, especially when the diagnosis depends on the existence of vascular flow. In such cases, the sonographic examination will be inconclusive, further imaging examinations will be required, which causes a delay in diagnosis. Superb microvascular imaging (SMI) is a novel vascular imaging mode, which provides visualization of low velocity and microvascular flow.(36)

SMI can detect tumor angiogenesis to distinguish thyroid nodules, and it has been shown to have a high diagnostic accuracy in differentiating benign from malignant thyroid nodules. It is an innovative Doppler ultrasound technology that uses adaptive algorithms to visualize micro vessels without contrast.(37)

SMI can display the blood flow of small vessels and low-velocity blood flow, which is difficult to visualize with conventional Doppler ultrasound.

SMI has been shown to have a high diagnostic accuracy in differentiating benign from malignant thyroid nodules.(38). In a recent study, the pooled the sensitivity, specificity, and positive and negative LR were 0.84, 0.86, 6.2, and 0.18, respectively.(37)

Traditional thyroid scanning using either [99mTc] pertechnetate or 123I can classify nodules as hyperfunctioning ('hot'), iso-functioning ('warm'), or hypo/non-functioning ('cold') when the serum thyrotropin (TSH) level is below normal or fine-needle aspiration cytology (FNAC) results are inconclusive. These radiotracers do not provide a definitive distinction between malignant and benign thyroid nodules. However, FDG-PET and [99mTc] Sestamibi scintigraphy, due to their high negative predictive values, can potentially reduce unnecessary thyroidectomies for thyroid nodules with uncertain cytology. The increased accessibility of FDG-PET or PET/CT has broadened the scope of radionuclide imaging, complementing the established radioiodine scans for the diagnosis, staging, and monitoring of thyroid cancer.(39)

As evidenced by this meta-analysis, blood flow dependent imaging techniques are superior in their abilities to be used as diagnostic tests, especially in conjunction with their use in detecting thyroid nodules. With ever increasing research breakthroughs, the use of techniques such as SMI, Radionuclide Scanning and Doppler Ultrasound will enhance diagnoses and management techniques.

Conclusions

In summary, this research paper provides a basis for further investigation into how radionuclide imaging, SMI and Color Doppler can be employed in the clinical diagnosis of thyroid nodules. It serves as a foundation for considering the use of radionuclide imaging as a diagnostic tool for thyroid nodules in clinical practice. It also indicates that SMI exhibits strong diagnostic precision in distinguishing between benign and malignant thyroid nodules and these findings propose the incorporation of SMI into the diagnostic process for thyroid nodules. The findings from this study can establish a theoretical foundation for the advancement and utilization of color doppler ultrasound technology in the clinical assessment of thyroid nodules. By amalgamating data for these imaging methods, sensitivity and specificity figures supported by a strong confidence interval of 95% were calculated. Thus, offering a starting point for delving into the utilization of these imaging methods in diagnosing thyroid nodules in a clinical setting.

Ethical Statement: Being a meta analysis, there were no ethical issues and IRB permission is not required.

Funding and Sponsorship: None of the authors have a financial interest in any of the products, devices, or drugs mentioned in this manuscript.

Conflicts of interest: The authors declare no conflict of interest.

References

1. Angell TE, Vyas CM, Medici M, Wang Z, Barletta JA, Benson CB, et al. Differential Growth Rates of Benign vs. Malignant Thyroid Nodules. J Clin Endocrinol Metab. 2017 Dec 1;102(12):4642–7.
2. Iqbal A, Rehman A. Thyroid Uptake and Scan. 2023.
3. English C, Casey R, Bell M, Bergin D, Murphy J. The Sonographic Features of the Thyroid Gland After Treatment with Radioiodine Therapy in Patients with Graves' Disease. Ultrasound Med Biol. 2016 Jan;42(1):60–7.
4. Xie C, Cox P, Taylor N, LaPorte S. Ultrasonography of thyroid nodules: a pictorial review. Insights Imaging. 2016 Feb 26;7(1):77–86.
5. The StayWell Company. The StayWell Company, LLC. 2022. What are thyroid nodules? Available from: https://www.cedars-sinai.org/health-library/diseases-and-conditions/t/thyroid-nodules.html
6. Vita R, Di Bari F, Perelli S, Capodicasa G, Benvenga S. Thyroid vascularization is an important ultrasonographic parameter in untreated Graves' disease patients. J Clin Transl Endocrinol. 2019 Mar;15:65–9.
7. Hiraiwa T, Tsujimoto N, Tanimoto K, Terasaki J, Amino N, Hanafusa T. Use of Color Doppler Ultrasonography to Measure Thyroid Blood Flow and Differentiate Graves' Disease from Painless Thyroiditis. Eur Thyroid J. 2013;

8. Dev Desai. Dev's Formulae for Diagnostic Test Accuracy Meta-analysis. medRxiv [Internet]. 2023 [cited 2023 Oct 7]; Available from: http://medrxiv.org/content/early/2023/03/27/2023.03.27.23287186.abstract
9. Basharat R, Bukhari MH, Saeed S, Hamid T. Comparison of fine needle aspiration cytology and thyroid scan in solitary thyroid nodule. Patholog Res Int. 2011;2011:754041.
10. Deandreis D, Al Ghuzlan A, Auperin A, Vielh P, Caillou B, Chami L, et al. Is (18)F-fluorodeoxyglucose-PET/CT useful for the presurgical characterization of thyroid nodules with indeterminate fine needle aspiration cytology? Thyroid. 2012 Feb;22(2):165–72.
11. Lin JH, Chiang FY, Lee KW, Ho KY, Kuo WR. The role of neck ultrasonography in thyroid cancer. Am J Otolaryngol. 2009;30(5):324–6.
12. Lumachi F, Varotto L, Borsato S, Tregnaghi A, Zucchetta P, Marzola MC, et al. Usefulness of 99mTc-pertechnetate scintigraphy and fine-needle aspiration cytology in patients with solitary thyroid nodules and thyroid cancer. Anticancer Res. 2004;24(4):2531–4.
13. Muñoz Pérez N, Villar del Moral JM, Muros Fuentes MA, López de la Torre M, Arcelus Martínez JI, Becerra Massare P, et al. Could 18F-FDG-PET/CT avoid unnecessary thyroidectomies in patients with cytological diagnosis of follicular neoplasm? Langenbecks Arch Surg. 2013 Jun;398(5):709–16.
14. Piccardo A, Puntoni M, Treglia G, Foppiani L, Bertagna F, Paparo F, et al. Thyroid nodules with indeterminate cytology: prospective comparison between 18F-FDG-PET/CT, multiparametric neck ultrasonography, 99mTc-MIBI scintigraphy and histology. Eur J Endocrinol. 2016 May;174(5):693–703.
15. Riazi A, Kalantarhormozi M, Nabipour I, Eghbali SS, Farzaneh M, Javadi H, et al. Technetium-99m methoxyisobutylisonitrile scintigraphy in the assessment of cold thyroid nodules: is it time to change the approach to the management of cold thyroid nodules? Nucl Med Commun. 2014 Jan;35(1):51–7.
16. Chen X, Wu CJ, Xing P, Chu YZ. Value of thyroid imaging-reporting and data system combined with shear wave elastography and superb microvascular imaging in the differentiation of benign and malignant thyroid nodules. J Harbin Med Univ. 2017;51(1):44–8.
17. Xuehong Diao JZLCJZCZYC. The value of superb micro-vascular imaging for diagnosis of thyroid nodules. Chinese Journal of Medical Ultrasound (Electronic Edition) [Internet]. 2016 Aug 1;13(08). Available from: {https://chaosheng.cma-cmc.com.cn/EN/10.3877/cma.j.issn.1672-6448.2016.08.013}
18. He GM LTZR. Value of ultrasonic strain elastography combined with ultra-fine blood flow classification in differentiating benign and malignant thyroid nodules. The Journal of Practical Medicine [Internet]. [cited 2023 Oct 11]; Available from: https://scholar.google.com/scholar_lookup?journal=J+Pract+Med&title=Value+of+ultrasonic+strain+elastography+combined+with+ultra-fine+blood+flow+classification+in+differentiating+benign+and+malignant+thyroid+nodules&author=GM+He&author=T+Li&author=RH+Zheng&volume=36&publication_year=2020&pages=1988-91&
19. Li YH, Wen DH, Li CX, Li XJ, Xue G. [The role of ATA (2015) guidelines, superb microvascular imaging, and spectral Doppler in differentiation between malignant and benign thyroid nodules]. Lin Chung Er Bi Yan Hou Tou Jing Wai Ke Za Zhi. 2017 Aug 5;31(15):1152–6.
20. Li Y GJSL. Application value of ultra vascular three-dimensional ultrasound imaging in differential diagnosis of benign and malignant thyroid nodules. Journal of Bengbu Medical College [Internet]. 2020 [cited 2023 Oct 11]; Available from: https://scholar.google.com/scholar_lookup?journal=J+Bengbu+Medical+Coll&title=Application+value+of+ultra+vascular+three-dimensional+ultrasound+imaging+in+differential+diagnosis+of+benign+and+malignant+thyroid+nodules&author=Y+Li&author=J+Guo&author=L+Su&volume=45&publication_year=2020&pages=507-10&
21. Pei S, Cong S, Zhang B, Liang C, Zhang L, Liu J, et al. Diagnostic value of multimodal ultrasound imaging in differentiating benign and malignant TI-RADS category 4 nodules. Int J Clin Oncol. 2019 Jun;24(6):632–9.
22. Wang Y ZDYF. Diagnostic value of ultramicro blood flow imaging and contrast-enhanced ultrasound in solid thyroid nodules. Chin Clin Oncol [Internet]. 2021 [cited 2023 Oct 11]; Available from: https://scholar.google.com/scholar_lookup?journal=Chin+J+Oncol&title=Diagnostic+value+of+ultramicro+blood+flow+imaging+and+contrast-enhanced+ultrasound+in+solid+thyroid+nodules&author=Y+Wang&author=D+Zhang&author=F+Yang&volume=48&publication_year=2021&pages=711-5&
23. Yang GX. The value of superb microvascular imaging for diagnosis of thyroid. Master's Thesis, Zunyi Medical University, Zunyi. 2017;
24. Zhao Y, Zhou P, Peng H, Liu W, Zhang Y, Lu X. [Application of superb microvascular imaging and contrast enhanced ultrasound in the differential diagnosis of thyroid nodules]. Zhong Nan Da Xue Xue Bao Yi Xue Ban. 2019 Jun 28;44(6):649–56.
25. Zhu YC, Zhang Y, Deng SH, Jiang Q. A Prospective Study to Compare Superb Microvascular Imaging with Grayscale Ultrasound and Color Doppler Flow Imaging of Vascular Distribution and Morphology in Thyroid Nodules. Med Sci Monit. 2018 Dec 19;24:9223–31.

26. Bozbora A, Erbil Y, Ozarmagan S, Barbaros U, Sari S, Degirmenci B. Color Doppler sonography in cold thyroid nodules for malignancy prediction. Acta Chir Belg. 2002 Aug;102(4):259–62.
27. Gannon AW, Langer JE, Bellah R, Ratcliffe S, Pizza J, Mostoufi-Moab S, et al. Diagnostic Accuracy of Ultrasound With Color Flow Doppler in Children With Thyroid Nodules. J Clin Endocrinol Metab. 2018 May 1;103(5):1958–65.
28. Gul K, Ersoy R, Dirikoc A, Korukluoglu B, Ersoy PE, Aydin R, et al. Ultrasonographic evaluation of thyroid nodules: comparison of ultrasonographic, cytological, and histopathological findings. Endocrine. 2009 Dec;36(3):464–72.
29. Li RQ, Yuan GH, Chen M, Shao YM, Zhu SN, Zhang JQ, et al. Evaluation of Diagnostic Efficiency of Ultrasound Features on Malignant Thyroid Nodules in Chinese Patients. Chin Med J (Engl). 2016 Aug 5;129(15):1784–8.
30. Lin JH, Chiang FY, Lee KW, Ho KY, Kuo WR. The role of neck ultrasonography in thyroid cancer. Am J Otolaryngol. 2009;30(5):324–6.
31. Ma J jiao, Ding H, Xu B hua, Xu C, Song L jun, Huang B jian, et al. Diagnostic performances of various gray-scale, color Doppler, and contrast-enhanced ultrasonography findings in predicting malignant thyroid nodules. Thyroid. 2014 Feb;24(2):355–63.
32. Palaniappan MK, Aiyappan SK, Ranga U. Role of Gray Scale, Color Doppler and Spectral Doppler in Differentiation Between Malignant and Benign Thyroid Nodules. J Clin Diagn Res. 2016 Aug;10(8):TC01-6.
33. Stacul F, Bertolotto M, De Gobbis F, Calderan L, Cioffi V, Romano A, et al. US, colour-Doppler US and fine-needle aspiration biopsy in the diagnosis of thyroid nodules. Radiol Med. 2007 Aug;112(5):751–62.
34. Durante C, Grani G, Lamartina L, Filetti S, Mandel SJ, Cooper DS. The Diagnosis and Management of Thyroid Nodules. JAMA. 2018 Mar 6;319(9):914.
35. Bartolotta TV, Midiri M, Galia M, Runza G, Attard M, Savoia G, et al. Qualitative and quantitative evaluation of solitary thyroid nodules with contrast-enhanced ultrasound: initial results. Eur Radiol. 2006 Oct 3;16(10):2234–41.
36. Jin H, Wang C, Jin X. Superb microvascular imaging for distinguishing thyroid nodules. Medicine. 2022 Jun 17;101(24):e29505.
37. Luo H, Yin L. Diagnostic value of superb microvascular imaging and color doppler for thyroid nodules: A meta-analysis. Front Oncol. 2023 Apr 5;13.
38. Artul S, Nseir W, Armaly Z, Soudack M. Superb Microvascular Imaging: Added Value and Novel Applications. J Clin Imaging Sci. 2017 Dec 28;7:45.
39. Iqbal A, Rehman A. Thyroid Uptake and Scan. 2023.